

Reversible Shrinkage of Giant Magnetoliposomes under an Osmotic Stress

C. Ménager* and V. Cabuil

Laboratoire Liquides Ioniques et Interfaces Chargées, UMR 7612, Université Pierre et Marie Curie, case 63, 4 place Jussieu, 75252 Paris Cedex 05, France

Received: October 25, 2001; In Final Form: May 29, 2002

Osmotic shrinkage of liposomes filled with a magnetic colloid (also called a ferrofluid) is described. Quantitative characterization of the shrinking process was performed by direct measurement of the vesicle radius as a function of the imposed osmotic pressure. Permeability of the 1,2-dioleoyl-*sn*-glycero-3-phosphocholine (DOPC) bilayer to water was calculated from the initial linear decrease of the radius with time. Spectacular shape modifications are also reported; the shrinking process leads to the formation of daughter vesicles as shown by optical microscopy. The reversibility of the osmotic shrinkage is proof of a neck connection between the daughter vesicles and the mother liposome. A phase transition of the magnetic colloid inside the liposome was observed in the last stage of the process.

One task of biological membranes is to maintain an osmotic equilibrium between the cytoplasm and the extracellular space. Biological membranes are much more permeable to water than to most other molecules (solute molecules, such as sugar and salts) and are therefore highly sensitive to osmotic gradients. For that purpose, most of them contain many ion pumps or ion channels to dampen the effect of an osmotic gradient. The osmotic equilibrium is thus determined by the concentration of macroions, such as hemoglobin or glucagene, which cannot cross over the hydrophobic barrier.

The regulation of the osmotic equilibrium has practical consequences, such as shape transitions. One of the most studied cases is the red blood cell, which exhibits various shapes depending on the osmolarity of the medium. Liposomes or vesicles are often used as models for biological cells because of their simplicity. They can shrink or swell by changing their volume according to the osmotic gradient. Osmotic swelling and shrinking have been studied for unilamellar vesicles using phase-contrast microscopy,¹ cryo-electron microscopy,² dynamic light scattering,³ and calorimetry.⁴ In a recent work,⁵ Evans et al. used micropipet aspiration to test the mechanical strength and water permeability of giant fluid bilayer vesicles composed of polyunsaturated phosphatidylcholine lipids.

In this paper, we describe the influence of an osmotic stress on giant liposomes filled with a magnetic colloid, or ferrofluid.⁶ Several aspects are discussed: (i) the osmotic deflating of a magnetoliposome in a hyperosmotic medium and its relation to the water permeability of the membrane, (ii) the shape modifications encountered by liposomes, and (iii) the reversibility of the observed phenomena. Finally, we report an original phase transition observed inside the liposome in the magnetic colloidal phase.

These results are discussed in terms of permeability and of pore formation, this latter point being important in the perspective of the use of magnetic particles as markers. Moreover, we show that the osmotic stress can be used to prepare liposomes with a high volume fraction of encapsulated magnetic particles.

Experimental Section

Materials. *The Phospholipid.* The phospholipid constituting the bilayer is 1,2-dioleoyl-*sn*-glycero-3-phosphocholine (DOPC, Sigma). Its phase transition temperature is $-22\text{ }^{\circ}\text{C}$ ⁷ so that the phospholipid molecules are always in a fluidlike state at room temperature. Because of a weak negative surface charge density caused by impurities,^{8–10} it is reasonable to suppose that there is no affinity between the negatively charged particles and the weakly negatively charged membrane.

The Magnetic Colloid. The magnetic colloid was a dispersion of citrate-coated maghemite ($\gamma\text{-Fe}_2\text{O}_3$) nanoparticles dispersed in water at pH 7 the synthesis of which is described elsewhere.¹¹ The volume fraction of maghemite oxide in water before encapsulation was 2%. The negative surface charges of the grains were ensured by the ionized trisodium citrate ligands (Na_3Cit). A residual ionic strength due to unadsorbed citrate species in equilibrium with the adsorbed ones was always present. It was monitored by dialysis through a cellulose membrane (Spectra/Por MWCO 12–14000, Roth France) and estimated by measurement of the conductivity of the ferrofluid.

Liposome Preparation. The preparation of giant liposomes encapsulating magnetic nanoparticles has already been described.^{12,13} As with the usual methods, it was based on the swelling of a phospholipidic film. But instead of starting the procedure with a dried lipid film, the lipid was prehydrated with the magnetic colloid. Thus an oily orange film was obtained, which was swollen thereafter with triply distilled water.

The procedure was as follows: 1 mg of dry DOPC powder was mixed with 10 μL of the aqueous dispersion (pH = 7, $[\text{Na}_3\text{Cit}] = c_0 = 3\text{ mM}$) of magnetic particles and sheared with a glove finger on a glass support (Petri dish) to obtain an oily orange film. Immediately after the shear, 1 mL of triply distilled water was poured onto the film to start the spontaneous swelling. The Petri dish was then placed in a water bath at $45\text{ }^{\circ}\text{C}$ for 20 min.

Determination of the Ionic Strength. The concentration of electrolyte (Na_3Cit) *outside* the liposomes was measured by conductimetry. The concentration *inside* the liposomes was first evaluated from the synthesis procedure and then verified before

* To whom correspondence should be addressed. E-mail: menager@ccr.jussieu.fr.

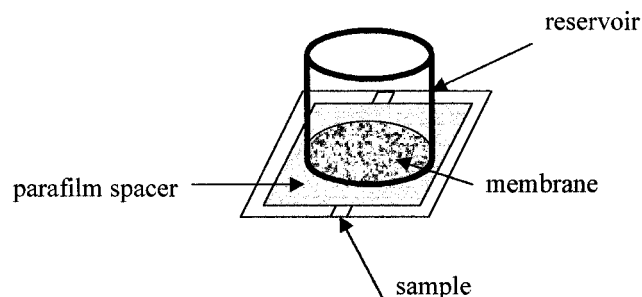


Figure 1. Schema of the customized cell.

the stress experiment. The conductivity of the magnetic colloid used for the preparation was $145 \mu\text{S}$, corresponding to a concentration of trisodium citrate equal to 3 mM . During the synthesis of the liposomes, a phospholipid lamellar phase filled with this salted solution was swollen by water. It is usually assumed that water diffuses through the phospholipid film (to form some opened structures). At this stage, there is an exchange between the future interior of the liposome and the water composing the surrounding medium. Diffusion of the nanometric particles was low enough to prevent a significant leak of the colloid into the swelling water and thus to allow a good encapsulation of the magnetic particles inside the liposomes. By comparison, the small citrate molecules diffuse much faster. In fact, the conductivity measurement (made with a conductometric microcell directly in the preparation after the swelling of the liposomes) gives a value of $3 \mu\text{S}$. This low conductivity is at the same level as the residual conductivity of water. Therefore, we cannot distinguish between a dilution of the sodium citrate electrolyte during the swelling process and a complete entrapment inside the liposomes. In this case, the osmotic equilibrium between the interior and the exterior was tested before each stress experiment by placing a solution of 3 mM citrate in the reservoir.

Determination of the Concentration of Magnetic Oxide inside the Liposomes. The measurement of the concentration of magnetic particles inside the liposomes by magnetophoresis has been described in a previous work.¹³ This concentration cannot be determined using a simple dilution factor for the above reason. The population of liposomes is heterogeneous in size and in color, indicating that the concentration of magnetic particles inside varies. For example, the biggest liposomes are certainly not the most concentrated ones.

Observation of the Samples. Magnetoliposomes were studied using an optical microscope (Zeiss 40x, NA 0.65); it was not necessary to use phase contrast because of the color given by the magnetic fluid encapsulated inside the liposomes. All observations and measurements were made on magnetoliposomes with diameters ranging between 20 and $60 \mu\text{m}$ and exhibiting thermal fluctuations of their membrane, which indicate that the membrane was made of one or two bilayers at the most. The sample was placed in a customized cell: the bottom plate was a cover-glass and the top one was a porous membrane Anodisc (Whatman) with $0.02 \mu\text{m}$ diameter pores. This setup enabled separation of the sample from the reservoir filled with the solution used to impose the osmotic stress (Figure 1). The reservoir was sealed to the membrane with paraffin. Samples were observed at room temperature, $21 \pm 2^\circ\text{C}$. Pictures from a charge-coupled device camera were recorded and digitized with a frame grabber (LG-3, Scion Corporation). The liposome diameter was measured as a function of time by using the Scion Image analysis software. Accuracy on the liposome volume was limited to a few percent.

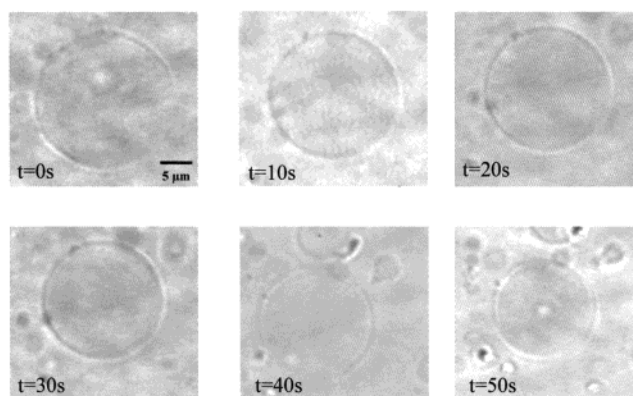


Figure 2. Optical microscopy of a magnetoliposome submitted to a concentration gradient of 21 mOsm . Time between two pictures is 10 s . The initial radius of the liposome is $12 \mu\text{m}$. The relative decrease of the vesicle radius is $\Delta R/R_0 = -0.3$. During the shrinkage, small vesicles are formed in the medium and stick to the liposome, but they are not expelled from it.

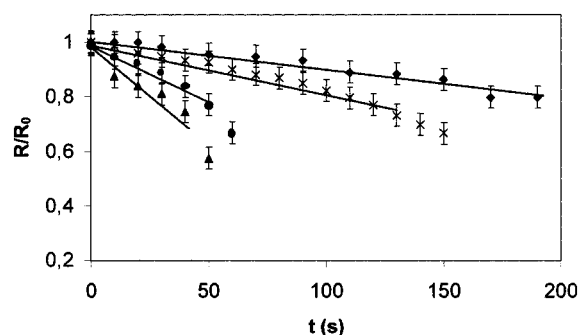


Figure 3. Plot of R/R_0 versus time (s) for several liposomes submitted to different concentration gradients: $\Delta c = (\blacklozenge)$ 21 , $(*)$ 51 , (\bullet) 110 , and (\blacktriangle) 216 mOsm . The drawn lines are guide for the eyes. The linear decay allows the determination of the permeability (see Table 2).

The Osmotic Stress Experiment. The magnetoliposomes were subjected to an osmotic stress by increasing the trisodium citrate concentration outside the liposomes. At the beginning of the experiment, a citrate solution of the same concentration as that used for the preparation ($c_0 = 3 \text{ mM}$) was placed in the reservoir. This allowed checking of the osmotic balance: no change in morphology and volume after 1 h at equilibrium was observed. Then the isoosmolar solution was removed, and citrate solution with the desired molarity was added. The concentration of the citrate solution (Na_3Cit) in the reservoir is denoted c_{ext} and ranges between 10 and 75 mM .

Results

Morphological Changes under an Osmotic Stress. Most of the liposomes prepared in this way were quasispherical with a radius R_0 , and their membranes exhibit thermal fluctuations. A few seconds after the addition of the hyperosmotic solution in the reservoir, a typical liposome begins to shrink, while fluctuations become more and more visible. Then its diameter suddenly decreases, as illustrated in Figure 2. The radius R is plotted as a function of time for several liposomes and four gradients of citrate concentrations between the reservoir and the liposome dispersion (Figure 3). The decrease, $\Delta R/R_0$, is on the order of -0.3 . The aspect of the colloidal solution inside the liposome does not change as long as the colloidal solution is stable.

The radius decreases linearly with time for about 1 min until the osmotic stress shrinks the liposome and the aspect of its interior begins to change: some daughter vesicles appear inside

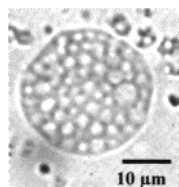


Figure 4. Optical microscopy of daughter vesicles superimposed to the projected area of the initial liposome. The liposome looks like a "raspberry".

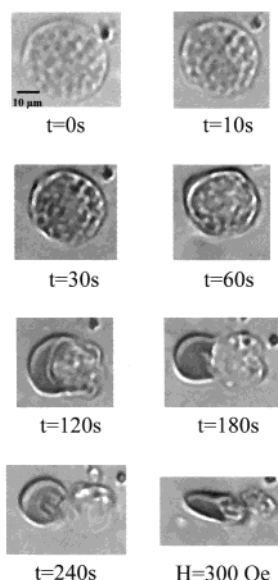


Figure 5. Evolution of the raspberry submitted to an osmotic stress. The inner phase becomes progressively denser and more and more contrasted. The invaginations are no more visible; the colloidal phase (the ferrofluid) separates from the rest of the liposome. At the end, we observe that the membrane sticks to a droplet of ferrofluid. This droplet exhibits a strong deformation as a magnetic field is applied.

the liposome (Figure 4). These microscopic vesicles appear progressively until the membrane is completely covered. At this stage the daughter vesicles are a few microns in diameter, and this corresponds to the points deviating from the linear decrease (Figure 3). The size of these daughter vesicles is not homogeneous, and their rate of formation is a function of the osmotic gradient. This second phase, which takes about 4 min, leads to a liposome that looks like a "raspberry".¹⁴ But the stress keeps on deflating the liposome and a reorganization of the colloidal phase (the ferrofluid one) inside the liposome can be observed (Figure 5). The ferrofluid phase appears more and more contrasted. At the end of the stress, the liposome appears as a concentrated drop of ferrofluid with a high volume fraction in magnetic particles, as shown by the deformation exhibited when a magnetic field of low intensity is applied (Figure 5). The droplet elongates in the field direction and the excess membrane reorganizes itself around this ferrofluid droplet.

To determine whether this phenomenon is reversible or not, shrinking experiments followed by reswelling were performed. At the end of the hyperosmotic stress experiment, water was placed in the reservoir instead of the citrate solution. The sequence is shown in Figure 6. The reswelling is not homogeneous at the beginning, but after about 1 h the liposome returns again to an almost spherical shape. However, the time scale of the reswelling (about 1 h) is not the same as that for the deflating (about 5 min). The membrane permeability to water cannot be measured during the reswelling because the aspect of the liposomes is no longer spherical.

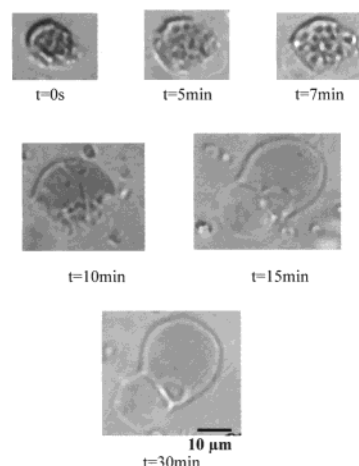


Figure 6. Beginning of the reswelling of a magnetoliposome that has been submitted to an osmotic stress. The recovery of an almost spherical shape is not shown here, the delay time is around 1 h.

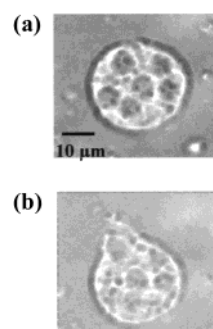


Figure 7. Formation of a macroscopic pore in the membrane. Panel a shows the presence of daughter vesicles linked to the liposome; panel b shows a hole opened in the membrane able to let the nanoparticles leak into the external medium.

During the shrinkage, no macroscopic holes were observed. However, when Δc is large (~ 70 mM), it is possible to induce a poration of the membrane, which allows leakage of the nanoparticles (Figure 7).

Permeability. When the external medium is hyperosmotic, the response of a liposome is to lose part of the water volume inside to equilibrate the osmolarity of the internal and external media. Quantitative characterization of the shrinking process has been performed by direct measurement of the vesicle radius as a function of concentration difference, Δc . Such measurements were only made when the liposome remained spherical and in the linear range described above. The osmotic pressure is related to the difference between the osmolarity of the internal medium (Osm_{int}) and the external medium (Osm_{ext}) by

$$\Delta\pi = RT(\text{Osm}_{\text{int}} - \text{Osm}_{\text{ext}})$$

The osmolarity of trisodium citrate solution at pH 7 was measured with a boiling point osmometer (Figure 8). In the range of salt concentration used here, the relation between the osmolarity and the concentration is $\text{Osm} = 3[\text{Na}_3\text{Cit}]$. The concentration of the citrate solution in the reservoir (c_{ext}) was varied from 10 to 75 mM. The value of $\Delta\text{Osm} = \text{Osm}_{\text{int}} - \text{Osm}_{\text{ext}}$ applied and the osmotic pressure, $\Delta\pi$, induced by the trisodium citrate solutions placed in the reservoir on top of the liposomes are given in Table 1. ΔOsm ranges from 21 to 216 mOsm, and the imposed pressure ranges then between 5×10^4 and 52×10^4 Pa (0.5 to 5 atm). The phospholipid membrane is semipermeable and much more permeable to water than to

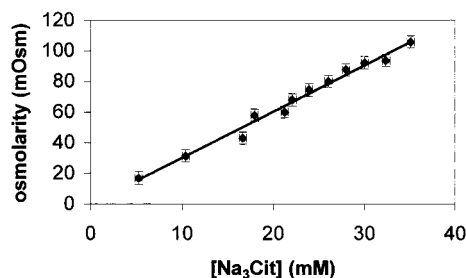


Figure 8. Osmolarity of trisodium citrate solution at pH 7 measured with a boiling point osmometer. The equation of the linear fit is $3.01[\text{Na}_3\text{Cit}] - 0.099$.

TABLE 1: Concentration of the Citrate Solutions Placed in Equilibrium with the Magnetoliposomes (c_{ext}) and Gradient (Δc) Calculated with the Initial Citrate Concentration of the Magnetic Fluid ($c_0 = 3 \text{ mM}$)

c_{ext} (mM)	10	20	40	75
Δc (mM)	7	17	37	72
ΔOsm (mOsm) ^a	21	51	110	216
$\Delta \pi$ ^b (Pa)	5×10^4	12×10^4	26×10^4	52×10^4

^a Milliosmolar equivalent is deduced from a calibration made with an osmometer. ^b The applied osmotic pressure gradient.

trisodium citrate (the citrate anions are large compared with the water molecules and highly charged). When exposed to a hyperosmotic medium, liposomes shrink because of a water flow toward the external medium. Thus, the permeability measured is due to water only through one or several bilayers, depending on the liposome.

The osmotic flow of water through a membrane is described by the equation¹⁵

$$J = -P\Delta c \quad (1)$$

where J is the molar flux density, Δc is the difference of molar concentrations between the aqueous solutions on both sides of the membrane, and P is the permeability (m/s). The theoretical background used for the interpretation of the osmotic stress is detailed in ref 1 and explained below. If we identify the instantaneous spherical surface area as seen under the microscope with the osmotically active area, we can write for a spherical vesicle of radius R

$$\frac{dR}{dt} = -\alpha P \Delta c \quad (2)$$

α being the molar volume of water. Equation 2 is associated with a linear decrease of R with time. It is in agreement with our observations. We computed the permeability P from the initial slope of the plot of R versus time for different liposomes and several gradients, $\Delta \pi$. The permeability of the DOPC bilayer to water obtained from the shrinking of several vesicles is listed in Table 2. Four of them are used in Figure 3 to confirm the linear decrease. Please note that the last points, which deviate from linear behavior, correspond to the beginning of the microscopic observation of the “raspberry”. The greater the gradient is, the faster the radius decreases.

For Δc equal to 216 mM, the uncertainty is important because the raspberry shape develops earlier than for the other gradients. Therefore, the permeability was calculated with only a few points at the beginning of the experiment. However, the measured permeability always ranges between 20 and 48 $\mu\text{m/s}$ with a mean value of $P = 34 \pm 7 \mu\text{m/s}$. The two values ($P = 19$ and $P = 20 \mu\text{m/s}$) were not taken into account because they probably belong to liposomes with a bilamellar wall, the

TABLE 2: Permeabilities, P , Calculated from Different Magnetoliposomes under an Osmotic Gradient, ΔOsm

R_0^a (μm)	ΔOsm (mOsm)	P ($\mu\text{m/s}$)
11.1	21	31
14.3	21	40
21.3	21	48
16	51	39.4
15	51	30
14.8	51	29
15.3	110	19
15.8	110	30
16.6	110	37
15.8	110	25
11.2	216	20
25	216	29

^a Initial radius of the liposome.

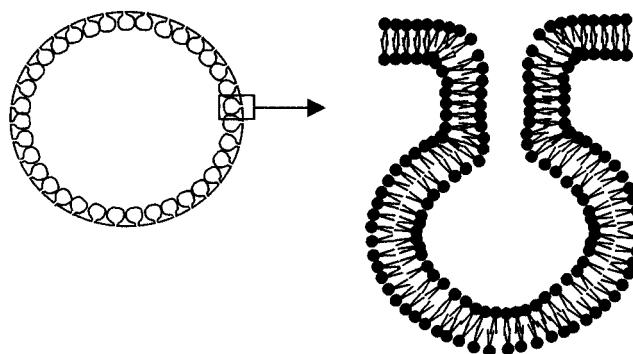


Figure 9. Schema of the “raspberry shape” and detail of the budding of the membrane toward the inner compartment of the vesicle.

permeability being almost half of a single bilayer. Sometimes fluctuating liposomes exhibit no shrinkage at all under the stress, perhaps because of the presence of permanent holes unresolved by optical microscopy.

Discussion

Raspberry Shape. A morphological change similar to that presented in Figure 4 has already been observed in the case of liposomes subjected to a gradient of glucose¹⁴ and named the “raspberry effect”. This phenomenon is related to the deflating of the liposome due to the volume change, the consequence being the existence of an excess of membrane. This excess membrane can induce the formation of daughter vesicles as is shown in Figure 4. Daughter vesicles are created from the budding of the membrane toward the inner compartment of the vesicle (Figure 9). It may be analogous to the endocytosis process in biomembranes. Note that such instabilities are not observed in the case of the micropipet method because the excess membrane is aspirated.

In the model proposed by Helfrich,¹ the spontaneous curvature is assumed to be caused by a lipid imbalance between the monolayers that is generated by a lipid flow parallel to the osmotic water flow. A variety of observations detailed in ref 1 indicate that osmosis induces a parallel lipid flow between the two monolayers of the bilayer, leading to a strong spontaneous curvature. As is illustrated in Figure 9, the formation of daughter vesicles implies a rearrangement of the phospholipid molecules leading to a large spontaneous curvature. Nevertheless, the so-called “raspberry effect” has not been observed in the case of the osmotic shrinkage of egg-lecithin vesicles,¹ perhaps due to the nature of the membrane. In fact, the DOPC bilayer is more flexible than the eggPC one, allowing the endocytosis process to be energetically favorable compared with the expulsion of daughter vesicles in the medium.

In their paper, Helfrich and co-workers ignore the shape of the postulated daughter vesicles. Two extreme forms are imagined: the sphere or the cylinder. Moreover, they ignored whether vesicles were still connected to the mother or not, in other words whether there is semifission or separation.

In the case of the magnetic liposomes, the reversibility of the osmotic shrinkage is evidence that a neck exists between the daughter vesicles and the mother vesicle. Even if the reversibility is not perfect, it is sufficient to state that there is no loss of membrane or at least it is not the predominant phenomenon. This assumption is confirmed in a recent work⁵ demonstrating the total recovery of volume after an osmotic stress.

Initial Linear Regime. As noted by Evans et al.,⁵ the values determined for water permeabilities differ significantly according to the type of experiment. In the literature, permeabilities are often measured on black lipidic films and are quoted between 17 and 100 $\mu\text{m/s}$,¹⁵ depending on the nature of the bilayer.¹⁶ We found a permeability of 34 $\mu\text{m/s}$ for DOPC bilayers, which is a realistic value for a single bilayer of DOPC. Recent contributions include Huster et al.¹⁷ giving a value of 123 $\mu\text{m/s}$ for permeabilities deduced from NMR spectroscopy on 100-nm-diameter vesicles made of DOPC at the same temperature. However, the value of ~ 34 $\mu\text{m/s}$ is in good agreement with the value found in ref 5 by the technique of micropipet aspiration (42 ± 6 $\mu\text{m/s}$) and with the value found in the pioneering work of Helfrich on EPC bilayers (40 $\mu\text{m/s}$).¹ This usual value of the permeability indicates that the nanoparticles inside the liposome do not disturb the properties of the membrane, in good agreement with ref 18 in which we demonstrated that the mechanical properties of the bilayer are not affected by the presence of the colloidal solution if the pH and the ionic strength of the solution are well controlled.

Shape in the Linear Regime. During the initial decrease of the vesicle radius, no destabilization of the membrane was optically observed. In fact, in our experiments, liposomes always preserve their apparent spherical shape as long as the decrease of the radius versus time is linear. During this initial and linear phase of the liposome shrinkage, and according to Figure 3, the liposome radius is reduced by 10–30%. Assuming that the liposomes remain spherical, this translates into an area change of 20–60%. Such large changes of liposome area can never be accommodated by lateral compression of the bilayer, so we must conclude, as did ref 1, that a loss of active wall area takes place during osmosis. The proposed mechanism, shown in ref 1 (which also explains the observation of protuberances growing out from multilamellar spherical vesicles) is the direct formation of daughter vesicles from the wall of the mother. However, in the initial linear range of the shrinkage, the daughter vesicles are smaller than the resolving power of the microscope. As proposed by Helfrich, this mechanism requires a correction of eq 2 assuming the formation of spherical daughter vesicles of constant radius r :

$$\frac{dR}{dt} \left(1 - \frac{2}{3} \frac{r}{R} \right) = -\alpha P \Delta c \quad (3)$$

For $r \ll R$, the corrected eq 3 reduces to the original eq 2, which justifies its use for the permeability evaluations. However, the small difference between eqs 2 and 3 can explain the deviation from the linear behavior as r becomes detectable. The mechanism of formation of daughter vesicles would be the same in the two ranges of shrinkage, but it is optically shown only in the second one, when the daughter vesicles are resolvable by optical microscopy.

Last Stage of the Shrinking Process. The difference between the system described here and the systems of refs 1 and 5 lies in the encapsulation of a colloidal solution inside the liposome. Please note that during all of these experiments, the osmotic pressure exerted by the particles is negligible compared with that exerted by the salt. Nevertheless, the presence of the encapsulated colloid should explain why, in the last stage of the shrinking process, the system never reached a plateau with an equilibrium radius. Instead of that, the magnetic colloid seems to concentrate and localize in a part of the structure as if it was undergoing a gas–liquid-like phase transition.¹⁹ It is difficult to precisely determine the volume fraction of magnetic particles in this phase, but its response to a magnetic field of 10^{-3} T indicates that it is very high, as in the concentrated liquidlike phase of a phase-separated sample. However, we can roughly evaluate it considering that, at a constant number of nanoparticles, the radius is reduced by a factor of 2. The volume fraction in magnetic particles is then multiplied by a factor of 8 leading to a volume fraction of 8% with an initial concentration of 1%. It is not surprising to induce such a phase separation, because the deflating process increases at the same time as the concentration of the colloid and the ionic strength. In this hypothesis, the shrinking process stops when the concentration of the colloid cannot increase any more.

Conclusion

This work confirms that the encapsulation of colloidal nanoparticles inside giant liposomes does not modify the properties of the lipid membrane, namely, here its permeability. We showed several years ago that the bending modulus K_c is not modified either. The colloidal dispersion acts as a contrast agent that allows visualization of the so-called “raspberry effect” when a giant liposome is subjected to an osmotic stress. It has to be underlined that in most cases the liposome membrane is not dramatically damaged and, more precisely, does not allow a release of nanometric species. Moreover, such an osmotic stress can be used to prepare highly magnetic liposomes, as is shown in the last stage of the process.

Acknowledgment. The authors thank Marie-Alice Guedeau-Boudeville and Olivier Sandre for helpful discussions.

References and Notes

- (1) Boroske, E.; Elwenspoek, M.; Helfrich, W. *Biophys. J.* **1981**, *34*, 95.
- (2) Mui B.; Cullis, P.; Evans, E.; Madden, D. *Biophys. J.* **1993**, *64*, 443.
- (3) Sun, S.-T.; Milon A.; Tanaka, T.; Ourisson G.; Nakatani, Y. *Biochim. Biophys. Acta* **1986**, *860*, 525.
- (4) Nebel, S.; Ganz, P.; Seelig, J. *Biochemistry* **1997**, *36*, 2853.
- (5) Olbrich, K.; Rawicz, W.; Needham, D.; Evans E. *Biophys. J.* **2000**, *79*, 321.
- (6) Rosensweig, R. E. *Ferrohydrodynamics*; Cambridge University Press: Cambridge, U.K., 1985.
- (7) Barton, P. G.; Gunstone, F. D., *J. Biol. Chem.* **1975**, *250*, 4479.
- (8) Carrion, F. J.; de la Maza, A.; Parra, J. L. *J. Colloid Interface Sci.* **1994**, *164*, 78.
- (9) Makino, K.; Yamada, T.; Kimura, M.; Oka, T. *Biophys. Chem.* **1991**, *41*, 175.
- (10) Pincet, F.; Cribier, S.; Perez, E. *Eur. Phys. J. B* **1999**, *11*, 127.
- (11) Massart, R. *IEEE Trans. Magn.* **1981**, *MAAG-17*, 1247.
- (12) Sandre, O.; Ménager, C.; Prost, J.; Cabuil, V.; Bacri, J.-C.; Cebers, A. In *Giant Vesicles*; Luisi, P. L., Walde, P., Eds.; John Wiley & Sons Ltd: Chichester, U.K., 2000; Chapter 11, pp 169–180.
- (13) Sandre, O.; Ménager, C.; Prost, J.; Cabuil, V.; Bacri, J.-C.; Cebers, A. *Phys. Rev. E* **2000**, *62*, 3865.

- (14) Guedeau-Boudeville, M.-A.; Bernard, A.-L.; Bradley, J.-C.; Singh, A.; Jullien, L. In *Giant Vesicles*; Luisi, P. L., Walde, P., Eds.; John Wiley & Sons Ltd: Chichester, U.K., 2000; Chapter 26, pp 341–349.
- (15) Tien, H. *Bilayer Lipid Membranes*; Marcel Dekker: New York, 1974.
- (16) Fettiplace, R. *Biochim. Biophys. Acta* **1978**, *513*, 1.
- (17) Huster, D.; Jin, A. J.; Arnold, K.; Gawrisch, K. *Biophys. J.* **1997**, *73*, 855.
- (18) Bacri, J. C.; Cabuil, V.; Cebers, A.; Ménager C.; Perzynski, R. *Europhys. Lett.* **1996**, *33*, 235.
- (19) Dubois, E.; Perzynski, R.; Boué, F.; Cabuil, V. *Langmuir* **2000**, *16*, 5617.